Available online at www.sciencedirect.com
ScienceDirect
Ceramics International 36 (2010) 871–877
CERAMICS INTERNATIONAL
www.elsevier.com/locate/ceramint

Hydrothermal synthesis of $NaNbO_3$ with low NaOH concentration

Shu Ya Wu *, Xiao Qiang Liu, Xiang Ming Chen

Department of Materials Science & Engineering, Zhejiang University, Hangzhou 310027, China

Received 22 April 2009; received in revised form 15 May 2009; accepted 3 October 2009
Available online 13 November 2009

Abstract

$NaNbO_3$ fine powders were prepared by reacting niobium pentoxide with low NaOH concentration solution under hydrothermal conditions at 160 °C. The reaction ruptured the corner-sharing of NbO_6 octahedra in the reactant Nb_2O_5, yielding various niobates, and the structure and composition of the niobates depended on the [OH^-] and reaction time. The fine Nb_2O_5 powder first aggregated to large particles and then turned to metastable intermediates with multifarious morphology. The reaction was fast for the situation of [OH^-] = 2 M. The [OH^-] determined the structure of final products, and three types of $NaNbO_3$ powder with the orthorhombic, tetragonal and cubic symmetries were obtained, respectively, depending on the [OH^-]. The low [OH^-] was propitious to yield orthorhombic $NaNbO_3$. The present work demonstrated that higher [OH^-] was not favored to synthesize $NaNbO_3$ powders and the conversion speed in this reaction was not in proportion to the [OH^-].

Keywords: A. Powders: Chemical preparation; B. Electron microscopy; B. X-ray methods; D. Niobates

1. Introduction

Alkaline niobates have attracted much scientific attention for their excellent nonlinear optical, ferroelectric, piezoelectric, electro-optic, ionic conductive, pyroelectric, photorefractive, selective ion exchange, and photocatalytic properties [1–17]. For example, lead-free potassium and sodium niobates are potential substitutes for lead zirconium titanate (PZT) as high-performance piezoelectric ceramics. Large lead content in piezoelectric PZT causes serious concerns about environment pollution during the fabrication, use and disposal of the materials, and therefore more and more attention has been paid to environmental issues nowadays, and research on the potential substitutes is more urgent than ever [3,16,17].

Alkaline niobate powders are usually synthesized by solid state reaction, where potassium salt and niobium pentoxide are heated at temperatures of 800 °C or above [8–10,16,17,19,27]. Sol–gel method using alkoxide and organic components as precusors has also been reported for synthesizing alkaline niobates. Cho synthesized (Na,K)NbO_3 thin films with chemical vapor deposition [2]. The synthesis of $KNbO_3$ has been widely investigated, while there are few papers on $NaNbO_3$ [3–6,8–11,16,18,23,24].

Currently, the hydrothermal synthesis of alkaline niobate powders has attracted much attention for its advantages, such as high degree of chemical homogeneity achieved on molecular scale, use of mild temperatures and pressures, a single step for the synthesis of nanocrystalline powders, and elimination of high-temperature calcination and ball-milling procedures [16,17,21,23–26]. C.H. Lu. et al. synthesized $KNbO_3$ with Nb_2O_5 particles at 200 °C in 8 M KOH solution [3]. I.C.M.S. Santos et al. obtained $NaNbO_3$ powders at 200 °C for 6–24 h with NaOH concentration between 4.3 and 8.4 M [4]. G.K.L. Goh. hydrothermally synthesized $NaNbO_3$ in NaOH solutions (6.7–15 M) at 150 °C and 200 °C [5]. J. Zhu synthesized $Na_2Nb_2O_6{\cdot}2/3H_2O$ fibers and $NaNbO_3$ cubes between 100 °C and 180 °C for a period of 30 min and 48 h in 10 M NaOH solution [8]. In the previous work on hydrothermal syntheses of $NaNbO_3$, all the reaction conditions involved high [OH^-], with the result that its liquid waste was very harmful to the environment. The reaction speed and mechanism in low [OH^-] remain unknown, and they are important issues.

In the present work, the influence of [OH^-] (1–4 M) on the product with various reaction times is systematically investigated in order to synthesize $NaNbO_3$ with low [OH^-]. The best [OH^-] to synthesize $NaNbO_3$ is discussed together with the key factors affecting the reaction speed.

* Corresponding author. Tel.: +86 571 87951410; fax: +86 571 87951410.
E-mail address: wushuya@zju.edu.cn (S.Y. Wu).

0272-8842/$36.00
doi:10.1016/j.ceramint.2009.11.006

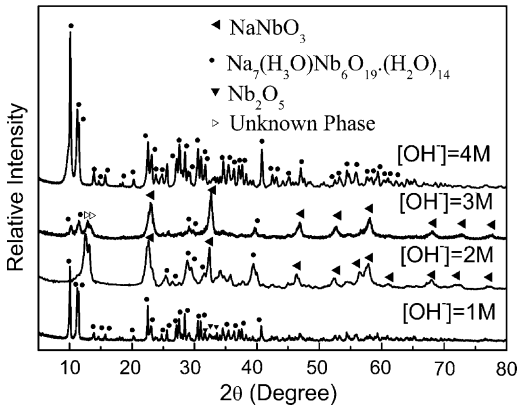

Fig. 1. XRD patterns of the powders prepared at 160 °C for 1.5 h with various OH^- concentration.

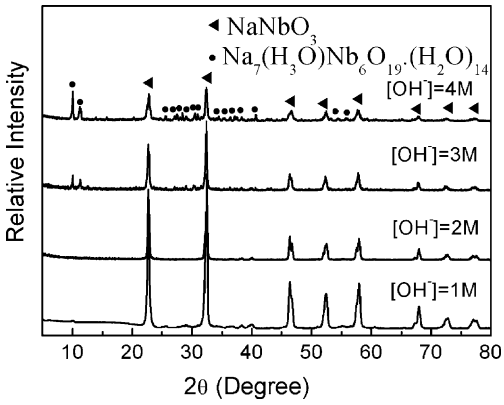

Fig. 2. XRD patterns of the powders prepared at 160 °C for 4 h with various OH^- concentration.

2. Experiments

Analytical grade sodium hydroxide (86%) and 4N niobium oxide were adopted as raw materials. Sodium hydroxide was dissolved in 150 ml distilled water and mixed with 0.01 mol Nb_2O_5. Hydrothermal synthesis of sodium niobate powders was conducted in a stainless steel autoclave of 200 cm^3 with a Teflon line under autogenous pressure. The resultant suspension was transferred to an autoclave with a filling factor of 80 vol%, and heated at 160 °C for 6 h. After cooling down, the solid residues were filtered and washed with distilled water until the pH value of filtrated solutions became 7–8. Finally, the product was poached ultrasonically with distilled water and dried at 80 °C in an oven.

The XRD analysis using Cu radiation (Rigaku D/MAX2550PC) was conducted to determine the crystal structure. The morphologies of the product powders were examined using a scanning electron microscope (XL-30-ESEM). Raman spectra of the product powders were measured by a Nicolet ALMEGA Raman spectrometer with the existing line at 523 nm of a Nd:YAG laser at room temperature. The exposure time of every sample was 1 s, and the number of exposure was 10 times. The thermal stability was investigated by TG–DTA with a heating rate of 10 °C/min.

3. Results and discussion

Fig. 1 shows the XRD patterns of the powders synthesized at 160 °C for 1.5 h with $[OH^-]$ = 1.0 M, 2.0 M, 3.0 M and 4.0 M. The content of $NaNbO_3$ phase first increases then decreases with increasing $[OH^-]$. When $[OH^-]$ is 1.0 M, the product is mainly composed of $Na_7(H_3O)Nb_6O_{19}\cdot(H_2O)_{14}$ and Nb_2O_5. The pattern of the powders obtained from the solution $[OH^-]$ = 2.0 M is different from the solution with

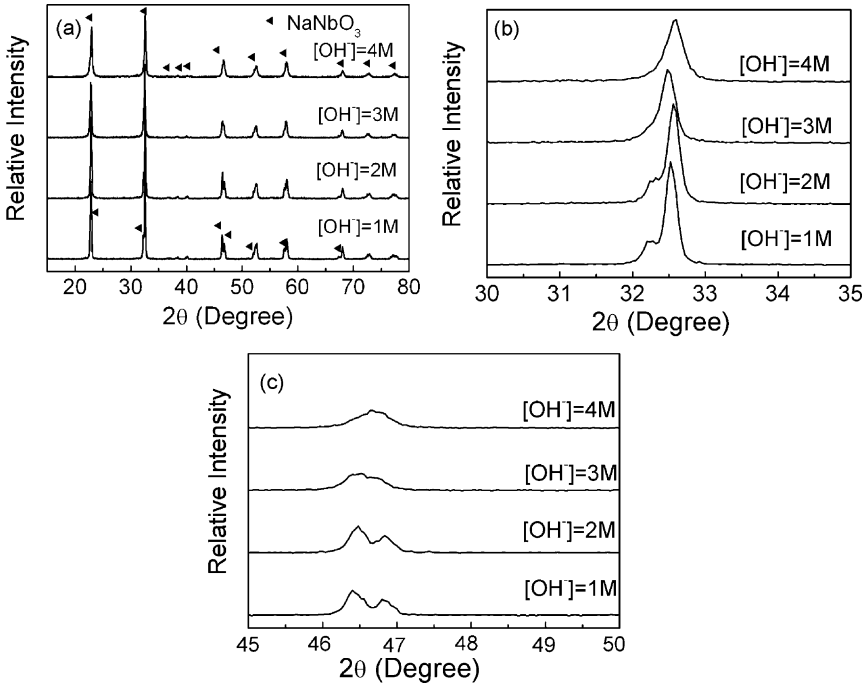

Fig. 3. XRD patterns of the powders prepared at 160 °C for 6 h with various OH^- concentration. (b and c) The enlarged views from (a).

$[OH^-]$ = 1.0 M where the $NaNbO_3$ phase is found in the patterns clearly, suggesting that the reaction between NaOH and Nb_2O_5 takes place more substantially. With increasing the $[OH^-]$ to 3.0 M, the conversion ratio of Nb_2O_5 increases, and the product is mainly of poorly crystallized $NaNbO_3$. The main product is also $Na_7(H_3O)Nb_6O_{19}{\cdot}(H_2O)_{14}$ when $[OH^-]$ is 4.0 M. Therefore, increase of the $[OH^-]$ does not accelerate its reaction speed, and it has the highest reaction speed for $[OH^-]$ = 3.0 M in 1.5 h.

The XRD patterns of the powders prepared after 4 h reaction at 160 °C with different $[OH^-]$ ($[OH^-]$ = 1.0 M, 2.0 M, 3.0 M and 4.0 M) are presented in Fig. 2. The product is almost $NaNbO_3$ for the situations of $[OH^-]$ = 3.0 M and 4.0 M. After being reacted with NaOH at 160 °C for 6 h, all the Nb_2O_5 powders have been transferred into $NaNbO_3$ (see Fig. 3). But $NaNbO_3$ derived from different solution has the different space groups. In $[OH^-]$ 1.0 M and 2.0 M solutions, the product is orthorhombic phase, and it is tetragonal when $[OH^-]$ is 3.0 M, and it becomes cubic phase when $[OH^-]$ increases to 4.0 M. According to the previous work, cubic $NaNbO_3$ (lueshite-type) could only be produced at temperatures below 100 °C, and increasing the hydrothermal temperature leads to the stabilization of solid-phase Nb_2O_5 (an undesirable phase) in acidic conditions as well as of aqueous species NbO_3^- at higher reagent concentrations, which diminishes the formation of $NaNbO_3$ [11]. However, we have synthesized the cubic at 160 °C, and it is much different from the literatures.

Fig. 4 is composition diagram of the samples synthesized at 160 °C with various OH^- concentration and various reaction time. It is obvious that excessive alkaline concentration is not necessary for acceleration of reaction. The optimal alkaline concentration for the fastest reaction is around $[OH^-]$ = 2 M. If there is plenty of OH^- in the precursor solution, the Nb_2O_5 slowly dissolves in the hydroxyl solution, and the OH^- also

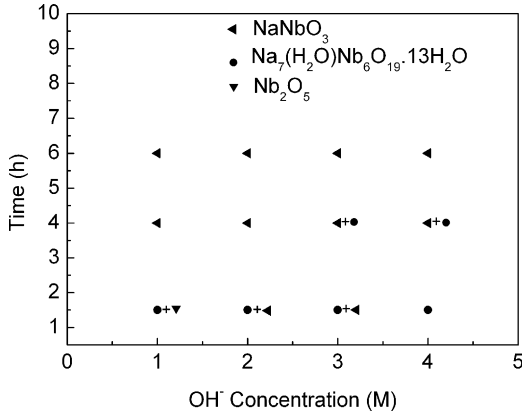

Fig. 4. Composition diagram of the samples synthesized at 160 °C with various OH^- concentration and various reaction time.

adsorbs in the surface of Nb_2O_5 powders, and there has an affinity between Nb = O bond and O–H bond, so Nb = O···OH···O = Nb forms under the hydrothermal condition. This helps to form entangled networks of polymeric chains of Nb hydroxides. The skeleton of the polymer corresponds to Nb atoms linked by bridging O atoms. Since an excess of sodium is always used and the sodium hydroxide has good solubility in water, Na^+ ions is very rich in the solution, and they adsorb at the surface of grains. The second stage of the synthesis is the crystallization of $Na_7(H_3O)Nb_6O_{19}{\cdot}(H_2O)_{14}$ by heating. As reported previously [20,22], $Nb_6O_{19}^{8-}$ hexaniobate Lindqvist ion, in which NbO_6 octahedrons share edges, is not very stable, so it changes to the stable $NaNbO_3$ perovskite, which has a NbO_3^- corner-sharing octrahedron network at higher temperature. The mechanism in NaOH–Nb_2O_5–H_2O system can be considered as following:

$$3Nb_2O_5 + 8OH^- \rightarrow Nb_6O_{19}^{8-} + 4H_2O \quad (1)$$

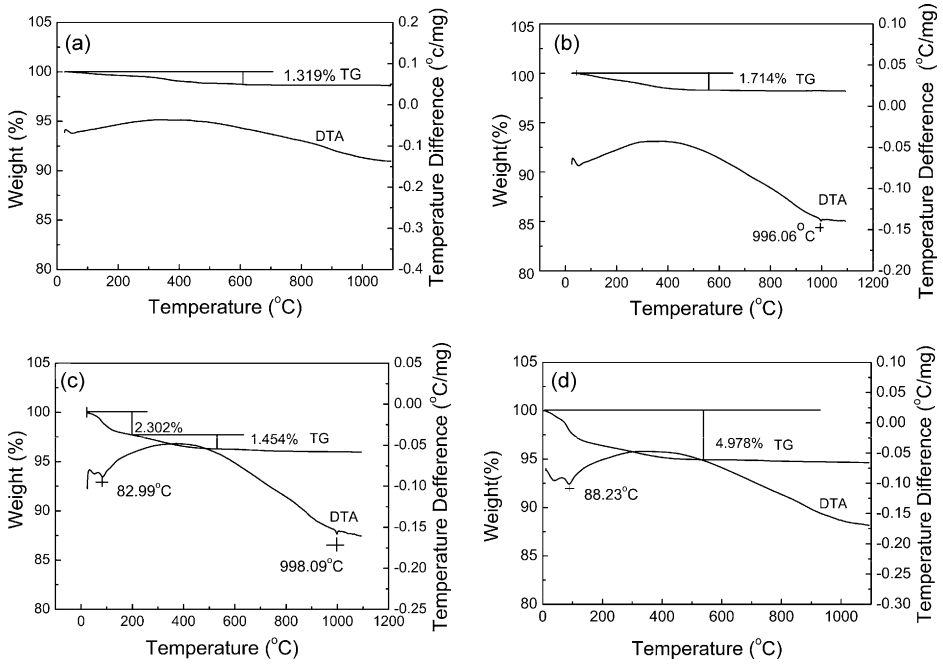

Fig. 5. DTA–TG curves of $NaNbO_3$ powders prepared at 160 °C for 6 h with various $[OH^-]$: (a) 1.0 M, (b) 2.0 M, (c) 3.0 M, and (d) 4.0 M.

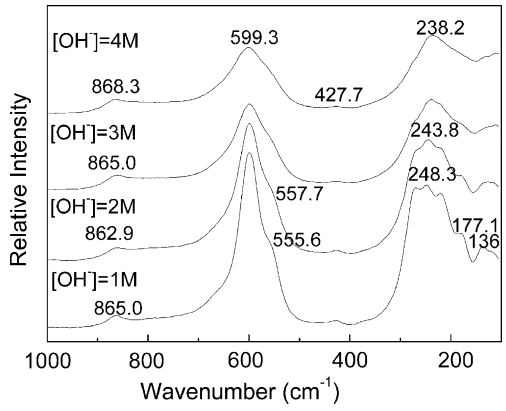

Fig. 6. Raman spectra of the powders prepared at 160 °C for 6 h with various OH^- concentration.

$$Nb_6O_{19}{}^{8-} + 7Na^+ + 16H_2O \rightarrow Na_7(H_3O)Nb_6O_{19}\cdot(H_2O)_{14}\downarrow + OH^- \quad (2)$$

$$Na_7(H_3O)Nb_6O_{19}\cdot(H_2O)_{14}\downarrow \rightarrow 6NaNbO_3\downarrow + Na^+ + OH^- + 15H_2O \quad (3)$$

The driving force of reaction (2) is provided by the supersaturation. The supersaturation can be defined as the ratio between the product of the current of concentration relevant aqueous species and the solubility product of $Na_7(H_3O)Nb_6O_{19}\cdot(H_2O)_{14}$. On the contrary, the concentration of the aqueous niobium species is related to the solubility of Nb_2O_5. Though the concentration of the aqueous species at the beginning of reaction is nearly constant because Nb_2O_5 is not dissolved in the cool hydroxyl solution, the niobium aqueous becomes different with increasing the reaction temperature. High [OH^-] is favor to dissolve Nb_2O_5 and form $Nb_6O_{19}{}^{8-}$. Since the reaction temperature is the same, the initial variation of supersaturation will be mainly related to the variation of niobium and sodium concentration, so reactions (1) and (2) are fast when there is high [OH^-]. Sodium is largely excessive in all the hydrothermal system, two much OH^- anions frustrated the reaction (3). So in higher [OH^-], reaction (3) is slower. The XRD patterns show equilibrium of the reactions (1)–(3) with various [OH^-] for different reaction time. [OH^-] is not the higher the better in preparing perovskite $NaNbO_3$.

As shown in Fig. 5, the difference between the orthorhombic and cubic structures is observed in the DTA–TG curves. The loss of mass increases with increasing [OH^-]. These results suggest that Na^+ ion in the crystal may be replaced partially with proton and this replacement induces adsorption of water. This is consistent with the previous result that as-synthesized powders of $KNbO_3$ included water molecules and OH^- [5]. A small peak is observed in the DTA curves in the solids synthesized with OH^- concentration of 2.0 M and 3.0 M, indicated there is a phase change.

The Raman spectrum of the powders synthesized for 6 h are shown in Fig. 6. The band positions of the Raman spectra provide important structure information of the samples. There is some difference among the samples synthesized with different [OH^-]. There is a shoulder peak about 555 cm^{-1} in the low [OH^-] sample, and it gradually disappears with increasing [OH^-]. There is a band in 872 cm^{-1} for all the samples, which should arise from the short Nb=O stretching mode (A_{1g}), and the band at 605 cm^{-1} can be assigned as the vibration mode of NbO_6 group (A_{1g}). The band at 563 cm^{-1} is the Nb–O–Nb stretching mode (E_g). The band at about 286 cm^{-1} arises from the breathing vibration of the ion Nb–O bonds bending mode (A_{1g}) [14,15,25]. It splits into three peaks in the orthorhombic structure, and they gradually become one peak. The Raman spectra are consistent with the structural information from XRD.

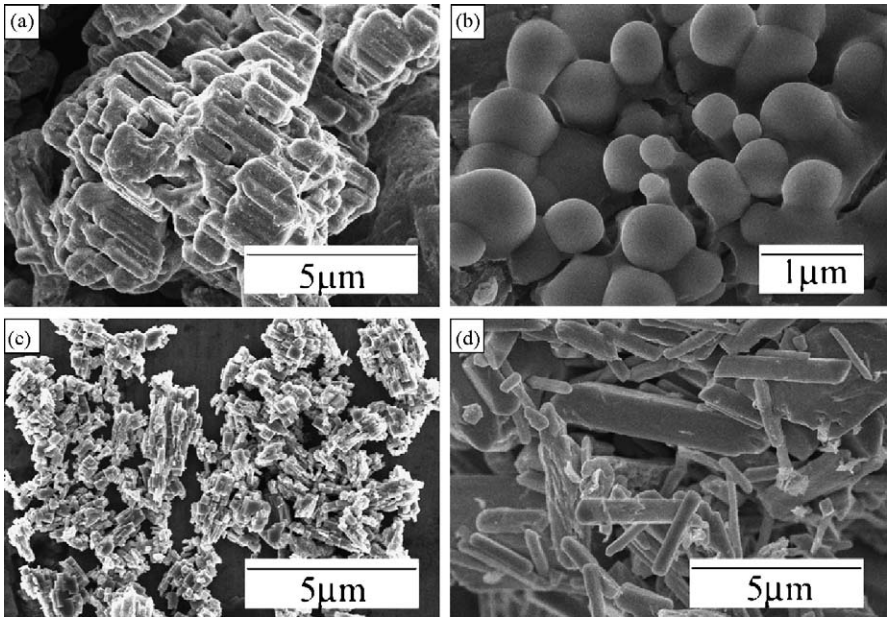

Fig. 7. SEM micrographs for powders prepared at 160 °C for 1.5 h from (a) [OH^-] = 1.0 M, (b) [OH^-] = 2.0 M, (c) [OH^-] = 3.0 M, and (d) [OH^-] =4.0 M solutions.

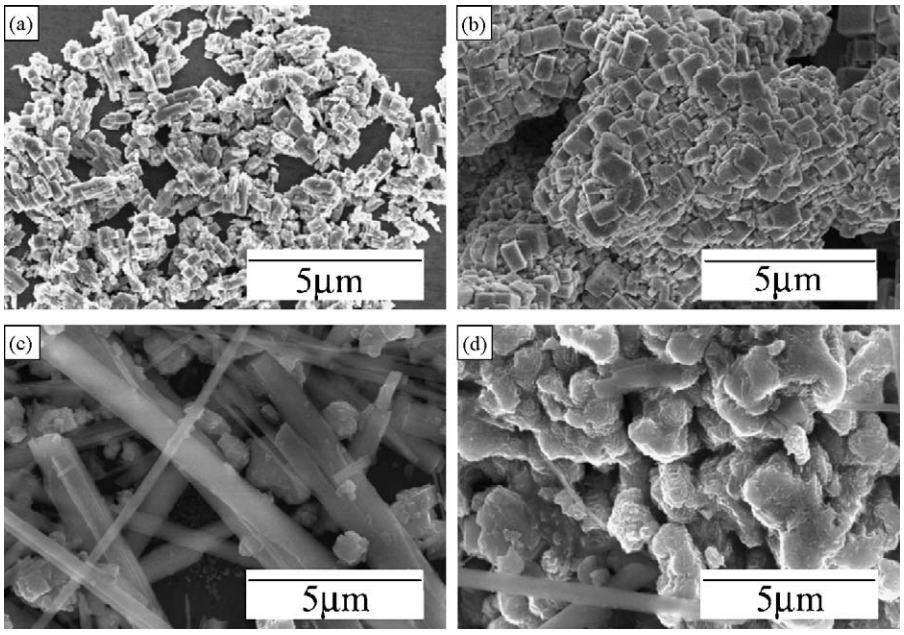

Fig. 8. SEM micrographs for powders prepared at 160 °C for 4.0 h from (a) [OH^-] = 1.0 M, (b) [OH^-] = 2.0 M, (c) [OH^-] = 3.0 M, and (d) [OH^-] = 4.0 M solutions.

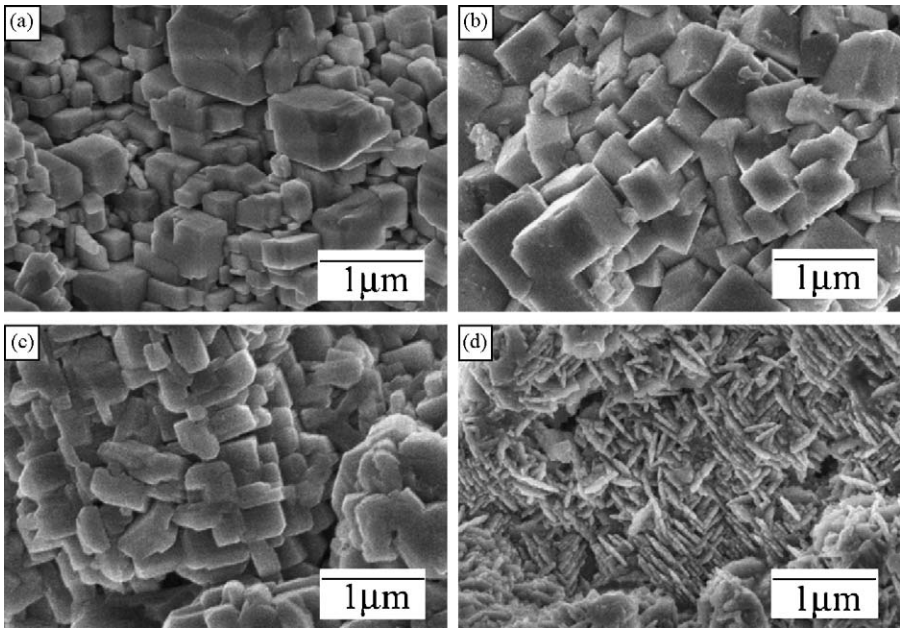

Fig. 9. SEM micrographs for powders prepared at 160 °C for 6.0 h from (a) [OH^-] = 1.0 M, (b) [OH^-] = 2.0 M, (c) [OH^-] = 3.0 M, and (d) [OH^-] = 4.0 M solutions.

SEM micrographs of the samples prepared at 160 °C for 1.5 h are shown in Fig. 7. The reactant Nb_2O_5 fine powders with a particle size of about 100 nm are observed in Fig. 6(a), and they react with the NaOH solution fast under hydrothermal conditions, yielding large grains of several micrometers in size in the early reaction in low [OH^-] (see Fig. 6(b)). The particles are highly porous which give a very high surface area in contact with the solution. When the [OH^-] is 2.0 M, the morphology of the particles is like mushroom. The new phase of the mushroom like particles observed in SEM images should be a sodium niobate, which coexists with the un-reacted Nb_2O_5. The reflection peaks in the XRD patterns of these mushroom like particles are broad and have low intensity, indicating poor crystallization in these mushroom-like solids. Cubic particles are observed when [OH^-] increases to 3.0 M, and bar-like s particles are obtained when [OH^-] is 4.0 M.

Fig. 8 shows SEM images of the samples synthesized at 160 °C for 4 h with varying [OH^-]: (a) 1.0 M, (b) 2.0 M, (c) 3.0 M, and (d) 4.0 M. The morphology is different at various [OH^-]. Image (a) shows cubic particles, and there are also the cubic particles in image (b) but they are smaller in size than those in image (a). When [OH^-] is 3.0 M, fiber like particles

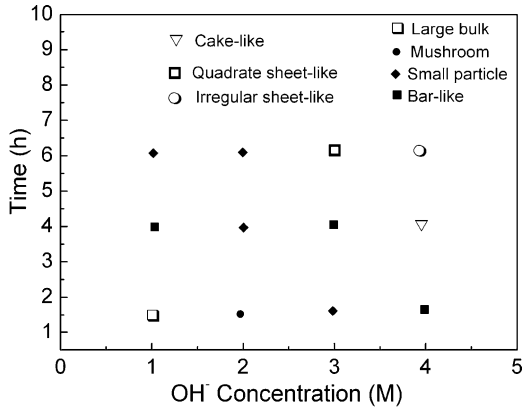

Fig. 10. Morphology diagram of the samples prepared at 160 °C with various OH^- concentration and various reaction time.

with porous grains are obtained. There are two morphologies in the image (d): the cake like particles, stacking with many layers is mixed with a few stick-like ones.

Fig. 9 shows the SEM images of the samples with (a) $[OH^-] = 1.0$ M, (b) $[OH^-] = 2.0$ M, (c) $[OH^-] = 3.0$ M, (d) $[OH^-] = 4.0$ M, after 6 h reaction at 160 °C. The morphology of (a) and (b) is almost the same. They are all cubic particles with the average sizes of 0.3 μm and 0.35 μm, respectively, and the particle size increases with increasing $[OH^-]$. With further increasing $[OH^-]$, the particles become thinner. When $[OH^-]$ is 3.0 M the particles are quadrate sheet-like, and the irregular sheet-like particles are observed for $[OH^-] = 4.0$ M.

Fig. 10 shows morphology diagram of the samples prepared at 160 °C with various OH-concentration and various reaction time. The morphologies of various intermediates are different at different alkaline concentrations based on the same reaction time. This is perhaps related with the draw and repulsive between cations and anions. When $[OH^-]$ is 1.0 M, after 4 h reaction, the component of the sample keeps unchanged, but change appears for its morphology. When $[OH^-]$ is 2.0 M, after 4 h reaction, no significant changes are identified for its component and morphology. The reaction is fastest at approximately $[OH^-] = 2$ M. The morphology of orthorhombic, tetragonal and cubic symmetries is different. That is, the $[OH^-]$ not only affects the products structure but also its morphology.

4. Conclusions

$NaNbO_3$ can be synthesized in low NaOH concentrations (1.0–4.0 M) at 160 °C. Three types of $NaNbO_3$ with the orthorhombic, tetragonal and cubic symmetries are obtained, depending on $[OH^-]$. The lower $[OH^-]$ is propitious to synthesize orthorhombic $NaNbO_3$. With increasing $[OH^-]$, it gradually turns to cubic. The reaction speed is controlled by the $[OH^-]$. Higher $[OH^-]$ is favorable to produce $Na_7(H_3O)Nb_6O_{19}.(H_2O)_{14}$, but too higher $[OH^-]$ can frustrate the formation of $NaNbO_3$, so the $[OH^-]$ is not the higher the better in synthesizing $NaNbO_3$. A small peak is observed in the DTA curves in the powders synthesized with $[OH^-]$ of 2.0 M and 3.0 M, and this indicates that there is a phase change. SEM micrographs provide a very interesting morphological change with the reaction condition. Different $[OH^-]$ leads to the intermediates with different morphologies. $[OH^-]$ also affects the product morphology. The $NaNbO_3$ powders with orthorhombic, tetragonal and cubic symmetries are cubic, square sheet-like and irregular sheet-like particles.

Acknowledgement

The present work was partially supported by Chinese National Key Project for Fundamental Researches under grant No. 2009CB623302.

References

[1] I. Nowak, M. Ziolek, Niobium compounds: preparation, characterization, and application in hereogeneous catalysis, Chem. Rev. 99 (1999) 3603–3624.
[2] C.R. Cho, c-Axis oriented (Na, K)NbO_3 thin films on Si substrates using metalorganic chemical vapor deposition, Mater. Lett. 57 (2002) 781–786.
[3] C.H. Lu, S.Y. Lo, H.C. Lin, Hydrothermal synthesis of nuclear optical potassium niobate ceramic powder, Mater. Lett. 34 (1998) 172–176.
[4] I.C.M.S. Santos, L.H. Lourerio, M.F.P. Silva, A.M.V. Cavaleiro, Studies on the hydrothermal synthesis of niobium oxides, Polyhedron 21 (2002) 2009–2015.
[5] G.K.L. Goh, F.F. Lange, S.M. Haile, C.G. Levi, Hydrothermal synthesis of $KNbO_3$ and $NaNbO_3$ powders, J. Mater. Res. 18 (2003) 338–345.
[6] C.H. Lin, C.H. Lee, J.H. Chao, Y.M. Huang, H.W. Chang, C.Y. Kuo, C.W. Hsu, A simple preparation procedure for the synthesis of sodium hexaniobate nanorods, Mater. Chem. Phys. 92 (2005) 128–133.
[7] J.M. Jehng, I.E. Wachs, Niobium oxide solution chemistry, J. Raman Spectr. 22 (1991) 83–89.
[8] J. Zhu, Z.F. Zheng, X.P. Gao, Y.N. Huang, Z.M. Yan, J. Zou, H.M. Yin, Q.D. Zou, S.H. Kable, J.C. Zhao, Y.F. Xi, W.N. Martens, R.L. Frost, Structural evolution in a hydrothermal reaction between Nb_2O_5 and NaOH solution: from Nb_2O_5 grains to micropotous $Na_2Nb_2O_6{\cdot}2/3H_2O$ fibers and $NaNbO_3$ cubes, J. Am. Chem. Soc. 128 (2006) 2373–2384.
[9] A. Magrez, E. Vasco, J.W. Seo, C. Dieker, N. Setter, L. Forro, Growth of single-crystalline $KNbO_3$ nanostructures, J. Phys. Chem. B 110 (2006) 56–58.
[10] M. Nyman, A. Tripathi, J.B. Parise, R.S. Maxwell, T.M. Nenoff, Sandia octahedral molecular sieves (SOMS): structural and property effects of charge-balancing the MIV-substituted (M = Ti, Zr) niobate framework, J. Am. Chem. Soc. 124 (2002) 1704–1713.
[11] A. Dias, V.S.T. Ciminelli, Electroceramic materials of tailored phase and morphology by hydrothermal technology, Chem. Mater. 15 (2003) 1344–1352.
[12] W.H. Nelson, R.S. Tobias, Structure of the polyanions of the transition metals in aqueous solution: the hexatantalate, Inorg. Chem. 2 (1963) 985–987.
[13] M. Posternak, R. Resta, A. Baldereschi, Role of covalent bonding in the polarization of perovskite oxides: the case of $KNbO_3$, Phys. Rev. B 50 (1994) 8911–8914.
[14] Y.P. Guo, K.I. Kakimotoand, H. Ohsato, Ferroelectric-relaxor behavior of $(Na_{0.5}K_{0.5})NbO_3$-based ceramics, J. Phys. Chem. Solids 65 (2004) 1831–1835.
[15] H. Abdelkefi, H. Khemahem, G. Velu, J.C. Carru, R.V. Muhll, Dilectric properties of ferroelectric ceramics derived from the system $BaTiO_3$-$NaNbO_3$-based solid solutions, Solid Stat. Sci. 6 (2004) 1347–1351.
[16] T. Zhong, J.L. Tang, M.K. Zhu, Y.D. Hou, H. Wang, H. Yan, Synthesis and characterization of layered niobate $K_4Nb_6O_{17}$ thin films by niobium-chelated precursor, J. Cryst. Growth 285 (2005) 201–207.
[17] M. Nyman, F. Bonhomme, T.M. Alam, M.A. Rodriguez, B.R. Cherry, J.L. Krumhansl, T.M. Neoff, A.M. Sattler, A general synthetic procedure for heteropolyniobates, Science 297 (2002) 996–998.

[18] L.A. Knauss, R. Pattnaik, J. Toulouse, Polarization dynamics in the mixed ferroelectric $KTa_{1-x}Nb_xO_3$, J. Phys. Rev. B 55 (1997) 3472–3479.
[19] F. Tessier, R. Assabaa, R. Marchand, Mixed valent niobium nitrides and oxynitrides resulting from ammonolysis of alkaline niobates, J. Alloys Compd. 262–263 (1997) 512–515.
[20] M. Filowitz, R.K.C. Ho, W.G. Klemperer, W. Shum, ^{17}O nuclear magnetic resonance spectroscopy of polyoxometalates. 1. Sensitivity and resolution, Inorg. Chem. 18 (1979) 93–107.
[21] A.V. Besserguenev, M.H. Dickman, M.T. Pope, Robust, alkali-stable, triscarbonyl metal derivatives of hexametalate anions, $[M_6O_{19}\{M'(CO)_3\}n]_{(8-n)}$ − (M = Nb, Ta; M′ = Mn, Re; n = 1,2), Inorg. Chem. 40 (2001) 2582–2586.
[22] P.L. Prater, L.L. Chase, L.A. Boatner, Raman scattering studies of the impurity-induced ferroelectric phase transition in $KTaO_3$:Nb, Phys. Rev. B 23 (1981) 221–231.
[23] S. Uchida, Y. Inoue, Y. Fujishiro, T. Sato, Hydrothermal synthesis of $K_4Nb_6O_{17}$, J. Mater. Sci. 33 (1998) 5125–5129.
[24] N. Miyamoto, T. Nakato, Liquid crystalline nature of $K_4Nb_6O_{17}$ nanosheet sols and their macroscopic alignment, Adv. Mater. 14 (2002) 1267–1270.
[25] K. Hegetschweiler, R.C. Finn, R.S. Rarig, J.J. Sander, S. Steinhauser, M. Worle, J. Zubieta, Surface complexation of $[Nb_6O_{19}]^{8-}$ with NiII: solvothermal synthesis and X-ray structural characterization of two novel heterometallic Ni-Nb-polyoxometalates, J. Inorg. Chim. Acta 337 (2002) 39–47.
[26] C.M. Flynn, G.D. Stucky, Heteropolyniobate complexes of manganese(IV) and nickel(IV), Inorg. Chem. 8 (1969) 332–334.
[27] T. Wada, K. Toyoike, Y. Imanaka, Y. Matsuo, Dielectric and pieoelectric properties of $(A_{0.5}Bi_{0.5})TiO_3$-$ANbO_3$(A = Na,K) systems, Jpn. J. Appl. Phys. 40 (2001) 5703–5705.